Chapter 9
Reactive Trace Gas and Aerosol Fluxes

Andreas Held, Malte Julian Deventer, Franz X. Meixner, Sebastian Schmitt, Matthias Sörgel, Linda Voß, and Veronika Wolff

9.1 Introduction

In addition to studying long-term carbon and water vapor fluxes (see Chap. 4), quantifying the surface-atmosphere exchange of reactive trace gases and aerosols is extremely important for a full understanding of biogeochemical cycles and

A. Held (✉)
Atmospheric Chemistry, University of Bayreuth, 95440, Bayreuth, Germany

Bayreuth Center of Ecology and Environmental Research, University of Bayreuth, Bayreuth, Germany
e-mail: andreas.held@uni-bayreuth.de

M.J. Deventer
Department of Geography, University of California, Berkeley, CA, 94720, USA

F.X. Meixner • M. Sörgel
Max Planck Institute for Chemistry, Hahn-Meitner-Weg 1, 55128 Mainz, Germany

S. Schmitt
Forschungszentrum Jülich, IEK-8, 52425 Jülich, Germany

L. Voß
GEO-NET Umweltconsulting GmbH, Große Pfahlstraße 5a, 30161 Hannover, Germany

V. Wolff
Agroscope, Reckenholzstrasse 191, 8046 Zürich, Switzerland

M. J. Deventer: Affiliation during the work at the Waldstein sites—University of Münster, Institut für Landschaftsökologie, Heisenbergstr. 2, 48149 Münster, Germany.

L. Voß, V. Wolff: Affiliation during the work at the Waldstein sites—Max Planck Institute for Chemistry, Hahn-Meitner-Weg 1, 55128 Mainz, Germany.

M. Sörgel, S. Schmitt: Affiliation during the work at the Waldstein sites—Atmospheric Chemistry, University of Bayreuth, 95440 Bayreuth, Germany.

A. Held: Affiliation during the work at the Waldstein sites before 2003—Department of Climatology, Bayreuth Institute of Terrestrial Ecosystem Research (BITÖK), University of Bayreuth, Germany.

T. Foken (ed.), *Energy and Matter Fluxes of a Spruce Forest Ecosystem*,
Ecological Studies 229, DOI 10.1007/978-3-319-49389-3_9

their implications for air quality and climate. For example, turbulent fluxes of nitric oxide (NO), nitrogen dioxide (NO_2), and ozone (O_3) as well as chemical reactions of the $NO/NO_2/O_3$ triad influence atmospheric ozone concentrations and thus oxidant budgets and the self-cleansing capacity of the atmosphere (see also Chap. 3). Atmospheric aerosol particles exhibit a direct climate effect due to scattering and absorption of radiation, and an indirect climate effect through aerosol-cloud interactions, which is currently considered the largest individual source of uncertainties in estimating the anthropogenic radiative forcing (Boucher et al. 2013).

Direct quantification of the turbulent exchange of reactive trace gases and aerosols by micrometeorological techniques is challenging for various reasons (see also Chap. 19): Firstly, both turbulence and chemistry contribute to changes in trace gas or aerosol concentrations. In particular, when the characteristic time scales of chemical reactions and turbulent transport are similar, it is difficult to separate chemical production or loss processes from turbulent transport. Secondly, for many trace gas and for aerosol measurements, fundamental assumptions required for valid flux measurements may be violated. For example, the aerosol number concentration cannot be considered a conservative scalar, and thus, the assumption of steady-state conditions required for direct eddy covariance measurements is violated under certain conditions. Thirdly, technical limitations of the available instrumentation for some trace gases and for size-resolved or chemically speciated aerosol measurements restrict their application in micrometeorological flux measurement techniques.

In this chapter, we will present flux measurements of reactive trace gases and aerosols carried out at the Waldstein-Weidenbrunnen site over the last 20 years. We will focus on ozone deposition and its implications for the $NO/NO_2/O_3$ triad, biogenic emissions of volatile organic compounds (VOC) from Norway spruce and their subsequent oxidation reactions, and, finally, the turbulent exchange of aerosol particles between a spruce canopy and the atmosphere.

In forest ecosystems such as the Waldstein site, dry deposition to the vegetation canopy is an important sink for tropospheric ozone (cf. Figure 9.1). The presence of tall vegetation significantly modifies the properties of the surface and thus the turbulent exchange conditions. Typically, the transport within the canopy is much slower than above the canopy, which provides additional time for chemical reactions in the canopy. In particular, ozone concentrations are closely linked to NO and NO_2, which play an important role in tropospheric chemistry. NO may be emitted from the forest soil and react with peroxy radicals to produce ozone. Depending on the ambient NO_2 concentrations, NO_2 may be taken up by the canopy (cf. Lerdau et al. 2000). Therefore, ozone exchange fluxes in a spruce forest such as the Waldstein site have to be evaluated in light of the chemical reactions of ozone with NO, NO_2, and other reactive nitrogen compounds such as nitrous acid (HONO; cf. Chap. 8).

Additional reaction partners for ozone at the Waldstein site include volatile organic compounds (VOC), in particular monoterpenes such as alpha-pinene. Emission strengths of biogenic VOC from Norway spruce are mainly dependent on temperature; however, emission patterns and strengths may change considerably depending on other factors such as plant age or environmental stress. Due to fast

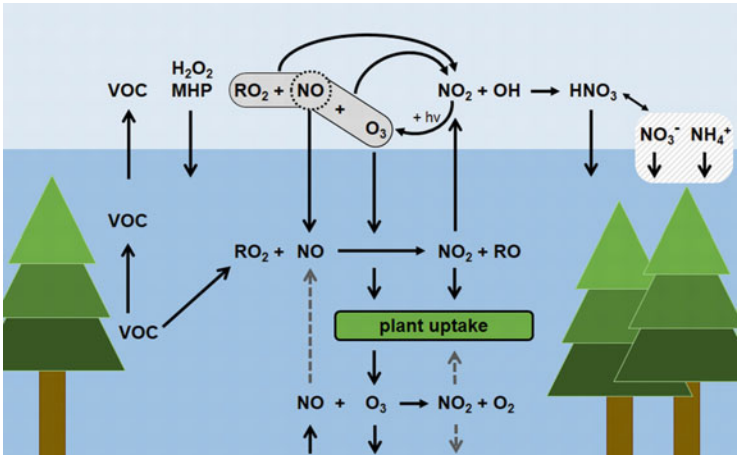

Fig. 9.1 Schematic representation of the trace gas fluxes above, within, and below the Waldstein spruce canopy

chemical reactions, branch emissions of volatile organic compounds may differ substantially from VOC exchange fluxes above the canopy. Both turbulent transport and chemical reactions of VOC have to be taken into account when quantifying the VOC budget in a forest ecosystem. Oxidation products of biogenic VOCs may partition into the particle phase, and thus, be an important source of new aerosol particles by gas-to-particle conversion.

The contribution of biogenic VOC oxidation products to new particle formation links the budgets of ozone, volatile organic compounds, and atmospheric aerosol particles at the Waldstein site. Turbulent transport may quickly remove freshly formed particles from the atmosphere. However, aerosol emission bursts and bidirectional aerosol fluxes, i.e., simultaneous emission of small particles and deposition of larger particles, have been observed at the Waldstein site. Climate and health effects of atmospheric aerosol particles depend strongly on aerosol concentration, size, chemical composition, and their spatial distribution in the atmosphere.

Close to the ground, number and mass concentrations and the spatial distribution of the atmospheric aerosol are determined to a large extent by surface-atmosphere exchange. Dry deposition can account for a large fraction of particle removal from the atmosphere. Directly measuring vertical aerosol fluxes, and thus quantifying dry deposition, is a prerequisite for a full understanding of the aerosol spatial distribution and associated environmental effects. While the contribution of vertical aerosol fluxes to the CO_2-dominated atmospheric carbon cycle can be considered insignificant, the net mass exchange of aerosol compounds such as sulfate and nitrate is important for the atmospheric sulfur and nitrogen cycles. Considering cloud formation and the number of cloud condensation nuclei, it is also important to evaluate whether forest canopies typically act as net sinks or net sources with respect to particle number. Therefore, improved and more comprehensive parameterizations

of vertical transport and exchange of aerosol particles in air quality and climate models are research priorities.

9.2 Materials and Methods

Direct micrometeorological flux measurements require fast-response sensors for the scalar of interest. For several trace gases such as ozone and nitrogen oxides, instrumentation has become available that is sufficiently fast for application in eddy covariance (EC) setups. However, for other trace gases such as nitric acid or organic peroxides, and for most aerosol properties, the measurement capabilities are limited with respect to time response. Therefore, if direct flux measurements are not possible due to technical limitations, indirect methods such as the aerodynamic gradient method (GRAD) or relaxed eddy accumulation (REA) are applied. In these methods, fluxes are derived from concentration differences measured at different heights or in updraft and downdraft samples collected by conditional sampling. Thus, GRAD and REA techniques require highly accurate and precise trace gas or aerosol instrumentation.

Most trace gas and aerosol flux measurements at the Waldstein-Weidenbrunnen site were carried out above the spruce canopy on top of the main tower at 32 m above ground level (agl). In dedicated field studies, additional flux measurements were made within and below the canopy. Many of the reactive trace gas and aerosol flux measurements presented in this chapter were carried out as part of large coordinated field experiments, either within the BEWA project or within the EGER project. The BEWA field experiments (Steinbrecher et al. 2004; Klemm et al. 2006) were conducted at the Waldstein site in the summers of 2001 and 2002, focusing on regional biogenic emissions of reactive volatile organic compounds (BVOC) from forests. The EGER project (Foken et al. 2012) studied exchange processes in mountainous regions in three intensive observation periods (IOP1/2/3) in the years 2007, 2008, and 2011.

For micrometeorological flux measurements of reactive trace gases and aerosols, combined measurements of the vertical wind speed (with a sonic anemometer) and the trace gas or aerosol concentration (with an appropriate analyzer) are required. In the following, the basic working principles of trace gas and aerosol analyzers, which have been applied in flux measurements at the Waldstein-Weidenbrunnen site, will be briefly summarized. For details about the full technical setup and data evaluation, the reader is referred to the literature.

9.2.1 Trace Gas Flux Instrumentation

Reactive trace gas flux measurements of ozone, nitrogen oxides, nitric acid, organic peroxides, and volatile organic compounds have been performed at the Waldstein-

Table 9.1 Instrumentation for reactive trace gas flux measurements at the Waldstein site

Trace gas	Principle of analyzer	Flux method	Reference
O_3	Solid-phase chemiluminescence	EC	Güsten and Heinrich (1996)
O_3	UV absorption	GRAD	Tsokankunku (2014)
NO/NO_2	Chemiluminescence	EC	Tsokankunku (2014)
NO/NO_2	Chemiluminescence	GRAD	Tsokankunku (2014)
HNO_3	NaCl denuder/ion chromatography (IC)	REA	Pryor et al. (2002)
Peroxides	Liquid chromatography with fluorescence detection (HPLC-FLD)	REA	Valverde-Canossa (2004)
VOC	Proton-transfer-reaction mass spectrometry (PTR-MS)	REA	Graus et al. (2006)
VOC	Gas chromatography with flame ionization detection (GC-FID)	REA	Steinbrecher et al. (2000)
VOC	Gas chromatography with mass spectrometry and flame ionization detection (GC-MS/FID)	REA	Schmitt (2013)

EC eddy covariance, *GRAD* aerodynamic gradient method, *REA* relaxed eddy accumulation

Weidenbrunnen site. Table 9.1 summarizes the applied trace gas analyzers and flux methods, which will be briefly explained in the following.

Fast-response ozone sensors based on solid-phase chemiluminescence (Güsten and Heinrich 1996) have been widely used in EC flux measurements of ozone. Ozone reacts with a dry chemiluminescent dye, and the resulting light intensity is proportional to the ozone concentration. There are various manufacturers of fast ozone sensors based on this principle, e.g., GFAS GmbH (Germany) or Enviscope GmbH (Germany). These sensors provide high-frequency (20 Hz) data of ozone fluctuations, however, no absolute ozone concentration measurements because of rapid degradation of the chemiluminescent dye, which changes the absolute sensitivity of the sensor for ozone. In order to derive ozone fluxes, ozone concentrations are measured side-by-side with slow-response ozone analyzers based on UV absorption.

For direct EC flux measurements of NO and NO_2, a fast two-channel NO/NO_2 analyzer (CLD 790SR-2, Eco Physics, Switzerland) was employed with a measuring frequency of 5 Hz. NO concentrations were quantified by the chemiluminescence reaction of NO with excess ozone: A certain fraction of the reaction product NO_2 will be in an excited state NO_2^*. NO_2^* returns to the ground state by photon emission, and these photons are then detected and counted. For NO_2 concentration measurements, NO_2 is converted to NO before the chemiluminescence measurement, which then yields the total concentration of NO and converted NO_2, i.e., NO_x. The concentration of NO_2 is calculated as the difference of the NO_x and the NO measurement, taking into account the efficiency of the NO_2 converter. For the flux measurements presented in Sect. 9.3.1, NO_2 was converted to NO with two blue light converters (AQD, MetCon GmbH, Germany) in series with a high

conversion efficiency. For calibration of the fast-response NO/NO_2 measurements, the concentrations were compared to a slow-response NO/NO_2 chemiluminescence analyzer (CLD TR-780, Eco Physics, Switzerland) measuring side-by-side.

For nitric acid (HNO_3) REA flux measurements (cf. Pryor et al. 2002), HNO_3 was sampled in one of three NaCl-coated denuders depending on the vertical wind speed: one for updrafts, one for downdrafts, and a third for constant sampling. The concentration difference of the updraft and downdraft sample was used for the REA approach, while the third denuder sample provided the average HNO_3 concentration for the entire measurement period. In order to increase the updraft/downdraft concentration differences, a dynamic dead band was applied. After HNO_3 sampling in the field, the denuders were extracted in deionized water and analyzed for NO_3^- by ion chromatography in the laboratory.

REA flux measurements of hydrogen peroxide and organic peroxides were conducted by collecting peroxides on two helix-shaped sampling coils depending on the vertical wind speed. The sampling coils were kept at a constant temperature of 5 °C, and deionized water acidified with H_3PO_4 was used as the scrubbing solution. Immediately after collection, the samples were analyzed by liquid chromatography (HPLC) with a fluorescence detector using post-column derivatization with horseradish peroxidase (Valverde-Canossa 2004).

Canopy-scale flux measurements of volatile organic compounds (VOC) require both sensitive and specific analyzers. Proton-transfer-reaction mass spectrometry (PTR-MS) is an extremely sensitive technique for the quantification of volatile organic compounds. The chemical ionization technique is based on proton transfer reactions from H_3O^+ reagent ions to volatile organic compounds (e.g., Lindinger et al. 1998). In the VOC flux measurements conducted during the BEWA field experiments, PTR-MS was applied in a REA setup. Meanwhile, the PTR-MS technique is sufficiently fast for application in direct EC flux measurements of VOC (e.g., Karl et al. 2001; Müller et al. 2010). In REA flux measurements, VOC analysis may also be performed by gas chromatography with flame ionization detection (GC-FID) or mass spectrometry (GC-MS). During the BEWA field experiments, VOC updraft and downdraft samples were collected depending on the vertical wind speed and separately directed to an online GC-FID system (HC1010, Airmotec, Germany). Details about the Airmotec VOC analysis including pre-concentration and cryo-focusing can be found in Steinbrecher et al. (2000). Schmitt (2013) utilized the GLOBOENET (Global Biogenic Organic Emissions Network) VOC REA sampler of the National Center for Atmospheric Research (NCAR, Boulder, CO, USA) to collect updraft and downdraft VOC samples on Tenax/Carbograph two-stage adsorbent tubes. Subsequently, the samples were sent to NCAR for offline analysis by thermal desorption GC-MS/FID for identification and quantification of isoprene and the five dominant monoterpene species.

9.2.2 Aerosol Flux Instrumentation

At the Waldstein-Weidenbrunnen site, measurements of net aerosol number fluxes, of size-resolved aerosol number fluxes, and of chemically speciated aerosol mass fluxes have been performed. The applied instruments and flux methods are summarized in Table 9.2. Further details about the aerosol instrumentation will be given in the following.

Aerosol number fluxes are frequently measured by eddy covariance with condensation particle counters (CPC), even though most commercially available CPCs are too slow for 10 Hz measurements due to the instrumental design with recirculation zones and laminar flow inside. In general, the aerosol sample enters a heated saturation chamber, which is typically saturated with butanol vapor. In a second step, both the particles and the butanol vapor enter a cooled condensation chamber, where the mixture becomes oversaturated with respect to butanol. This leads to condensation of butanol on particles with diameters as small as 3 nm (cf. Table 9.2) and rapid growth of these particles. Finally, the grown particles are individually detected and counted by light scattering.

In order to increase the time response of the CPC measurement, Wehner et al. (2011) built a fast mixing-type CPC (Fast CPC), where butanol-saturated air is mixed with the aerosol sample in a small mixing volume. Similar to laminar flow CPCs, the lower cutoff diameter depends on the temperature difference between the saturator temperature and the condenser temperature. In the Fast CPC used at the Waldstein site, this diameter varied between 6.4 nm and 9.9 nm. In a characterization experiment, Wehner et al. (2011) report an e-folding response time of 5 ms for their Fast CPC.

For size-resolved aerosol number flux measurements, an electrical low pressure impactor (ELPI+, Dekati Ltd., Finland) was applied. In the ELPI+ aerosol spectrometer, particles are electrically charged by corona discharge and separated according to their aerodynamic diameter in a 13-stage cascade impactor (17 nm to 10 μm) and a backup filter stage (6–17 nm). When the charged particles are collected on the impaction plates, they produce a current, which is proportional to the total particle concentration of the respective size fraction. The currents are measured individually using 14 electrometers with a measuring frequency of 10 Hz.

Total ammonium and nitrate fluxes (including both gas and particle phases) were derived from concentration measurements at two heights (30.9 m and 24.4 m agl) above the canopy with a wet chemical instrument, the gradient of aerosol and gases online registrator (GRAEGOR, ECN Petten, Netherlands). Gas and particle samples are collected simultaneously at two heights with a pair of wet annular denuders and steam-jet aerosol collectors, respectively. In the denuders, water-soluble gases diffuse into the sample solution.

Table 9.2 Instrumentation for aerosol flux measurements at the Waldstein site

Flux target	Instrument	Manufacturer	Diameter range	Flux method	Reference
Net aerosol number	CPC 3760A	TSI Inc. (USA)	>11 nm	EC	Held and Klemm (2006)
Net aerosol number	UCPC 3025	TSI Inc. (USA)	>3 nm	EC	Held and Klemm (2006)
Net aerosol number	Fast CPC	Custom-built (Wehner et al. 2011)	>6.4 nm	EC	Kittler F., personal communication
Size-resolved aerosol number	ELPI+	Dekati Ltd. (Finland)	6 nm to 10 μm	EC	Deventer et al. (2015)
Chemically speciated aerosol mass	GRAEGOR	ECN Petten (Netherlands)	Not specified	GRAD	Wolff et al. (2010a, 2010b)
Chemically speciated aerosol mass	LAMPAS2	Custom-built (Trimborn et al. 2000)	200 nm to 10 μm	IDES	Held et al. (2003)

CPC condensation particle counter, *UCPC* ultrafine condensation particle counter, *ELPI* electrical low pressure impactor, *GRAEGOR* gradient of aerosol and gases online registrator, *LAMPAS* laser mass analyzer for particles in the airborne state, *EC* eddy covariance, *GRAD* aerodynamic gradient method, *IDES* irregular disjunct eddy sampling

Subsequently, the sample air is mixed with a supersaturated flow of deionized water vapor in the steam-jet aerosol collector. Due to water vapor condensation, the particles rapidly grow to droplets, which are collected in a cyclone. Finally, the denuder sample solution (containing the dissolved gas-phase species) and the cyclone solution (containing the dissolved particulate species) are sequentially analyzed for anions using ion chromatography (IC) and for NH_3/NH_4^+ using flow injection analysis (FIA).

Held et al. (2003) presented the first approach to combine aerosol mass spectrometry and a micrometeorological technique to derive chemically speciated aerosol fluxes. The aerosol mass spectrometer LAMPAS2 (Laser Mass Analyzer for Particles in the Airborne State; Trimborn et al. 2000) ionizes individual aerosol particles by laser desorption ionization. Individual particles are hit by a pulsed ionization laser, which leads to (partial) vaporization and ionization. The resulting positive and negative ions are analyzed with a bipolar time-of-flight mass spectrometer, which yields information about the chemical composition of this individual particle. Because the exact sampling time of each analyzed particle is known, the corresponding vertical wind speed can be attributed to each individual particle composition in a post-processing step, and virtual conditional sampling is possible. Due to the fact that the timing of the aerosol analysis is irregular, this approach was called irregular disjunct eddy sampling (IDES).

9.3 Results and Discussion

A large number of reactive trace gas and aerosol flux measurements have been carried out at the Waldstein-Weidenbrunnen site over the last 20 years. Firstly, flux measurements of the $NO/NO_2/O_3$ triad and related flux measurements of HNO_3, organic peroxides, and volatile organic compounds will be summarized. Then, total and size-resolved aerosol number fluxes and chemically speciated aerosol mass fluxes will be presented and discussed. Finally, the observed fluxes will be compared with various parameterizations of turbulent transport and coupled chemistry-transport models.

9.3.1 Reactive Trace Gas Flux Measurements

In forest ecosystems such as the Waldstein site, dry deposition to the vegetation canopy is an important sink for trace gases such as ozone.

9.3.1.1 Ozone Fluxes

Turbulent deposition fluxes of ozone have been measured by eddy covariance since the late 1990s at the Waldstein-Weidenbrunnen site. Klemm and Mangold (2001) report ozone deposition fluxes varying from roughly −3 to −14 nmol m^{-2} s^{-1} on a daily average basis. In a more detailed analysis of the diurnal cycle of ozone deposition fluxes, the median flux values range from −0.5 to −8.6 nmol m^{-2} s^{-1} (Klemm et al. 2004). Klemm et al. (2004) also compared ozone fluxes measured above and below the canopy (at 32 m and 3 m agl) during the BEWA field campaign. The ozone flux ratio above/below the canopy ranged from 3.3 to 8.9.

This is consistent with Tsokankunku (2014), who obtained ozone deposition fluxes up to −25 nmol m^{-2} s^{-1} above the canopy and up to −2.5 nmol m^{-2} s^{-1} below the canopy, from eddy covariance measurements during EGER IOP2. However, ozone fluxes derived from a gradient approach for the same period ranged from −10 nmol m^{-2} s^{-1} to +10 nmol m^{-2} s^{-1} above the canopy and up to −2.5 nmol m^{-2} s^{-1} below the canopy. Obviously, the discrepancy between the eddy covariance and gradient methods above the canopy indicates a nonuniform distribution of ozone sources and sinks across the canopy.

Zhu et al. (2009) compared ozone fluxes measured at three different levels, above, within, and below the canopy (32 m, 17 m, 1 m agl) during EGER IOP2. During the day, the mean ozone flux was −11.0 nmol m^{-2} s^{-1} above the canopy, −7.0 nmol m^{-2} s^{-1} within the canopy, and −0.8 nmol m^{-2} s^{-1} below the canopy. At night, the mean ozone flux was −5.2 nmol m^{-2} s^{-1} above the canopy, −3.2 nmol m^{-2} s^{-1} within the canopy, and −0.5 nmol m^{-2} s^{-1} below the canopy. This indicates that ozone deposition in the layer from 1 m to 17 m agl contributes most to the total deposition (about 54 %), while the layer below 1 m agl contributes about 8 %, and the layer from 17 m to 32 m agl contributes roughly 38 % to the total deposition flux on a daily mean basis.

During EGER IOP3, Voß (2015) analyzed ozone fluxes measured at the Waldstein-Weidenbrunnen site above the undisturbed canopy (32 m agl) and at 5.5 m agl about 280 m south of the main tower at the Köhlerloh clearing, representing a disturbed part of the ecosystem. They calculated median ozone deposition fluxes of −13 nmol m^{-2} s^{-1} above the canopy and −7.5 nmol m^{-2} s^{-1} at the clearing, with distinct diurnal patterns and the highest absolute values during daytime. This diurnal variation indicates stomatal activity as an important controlling factor. However, the observed nighttime deposition suggests that additional ozone sinks exist. A comparison of the ozone deposition fluxes in the undisturbed and disturbed parts of the ecosystem shows that a reduction of the vegetation, e.g., by wind disturbances, is also reflected in reduced ozone deposition fluxes equivalent to the ratio of the leaf area indices of the canopies before and after the disturbance.

Evidently, during advection and vertical transport within the canopy, there is time for chemical reactions. Ozone concentrations are closely linked to concentrations of NO and NO_2 through reactions R9.1–R9.3:

$$O_3 + NO \rightarrow NO_2 + O_2 \quad \text{(R9.1)}$$

$$NO_2 + h\nu \rightarrow NO + O \quad \text{(R9.2)}$$

$$O + O_2 + M \rightarrow O_3 + M \quad \text{(R9.3)}$$

The effectiveness of R9.1 as a sink for ozone depends on the spatial distribution of O_3 and NO sources and the transport of these compounds. If NO is emitted from the soil and ozone mixed into the canopy from aloft, R9.1 may be limited when turbulent mixing is not active or when the sub-canopy is vertically decoupled from above-canopy layers (cf. Chap. 6). The production of ozone by R9.2 and R9.3 mainly depends on the photolysis rate of NO_2, which is considerably reduced below the canopy. Therefore, the chemical reactions of ozone with NO, NO_2, and other reactive compounds have to be taken into account when evaluating ozone exchange fluxes within and above the canopy.

9.3.1.2 NO_x Fluxes

NO and NO_2 fluxes were measured by eddy covariance and compared with a gradient approach during EGER IOP2 (Tsokankunku 2014). NO fluxes above the canopy were directed toward the surface and ranged up to -1.75 nmol m^{-2} s^{-1} both in the eddy covariance and the gradient flux measurements. In contrast, NO_2 eddy covariance fluxes were positive from 0 to $+2$ nmol m^{-2} s^{-1}, whereas NO_2 fluxes obtained from the gradient method ranged from -2 to $+2$ nmol m^{-2} s^{-1}. With the gradient method, NO/NO_2 fluxes were also calculated below the canopy close to the ground. Here, NO fluxes were positive from $+0.1$ to $+0.45$ nmol m^{-2} s^{-1}, which reflects NO soil emissions. NO_2 fluxes ranged from -0.2 to $+0.3$ nmol m^{-2} s^{-1}.

Breuninger et al. (2012, 2013) obtained exchange fluxes of NO and NO_2 between the spruce canopy and the atmosphere from dynamic chamber measurements at the branch level. During daytime, nitrogen oxide exchange fluxes were mostly directed toward the vegetation surface (NO, -0.110 to $+0.090$ nmol m^{-2} s^{-1}; NO_2, -0.341 to $+0.058$ nmol m^{-2} s^{-1}). At night, NO exchange fluxes were exclusively positive ($+0.002$ to $+0.023$ nmol m^{-2} s^{-1}), while NO_2 exchange fluxes were still mostly negative (-0.414 to $+0.155$ nmol m^{-2} s^{-1}). At the same time, ozone exchange fluxes were almost exclusively directed toward the vegetation surface (-1.167 to $+0.293$ nmol m^{-2} s^{-1}). Interestingly, the NO_2 compensation point concentrations,

i.e., the NO_2 concentration above which the canopy acts as a net NO_2 sink and below which the canopy acts as a net NO_2 source, calculated from these data were not significantly different from zero, thus challenging the existence of a NO_2 compensation point concentration for spruce.

Table 9.3 summarizes trace gas fluxes of ozone and nitrogen oxides observed at the Waldstein site. Ozone fluxes are mostly negative, i.e., directed toward the surface. Ozone deposition is typically higher during the day and reduced to about 50 % at night, which is consistent with reduced stomatal uptake when stomata are closed (Foken et al. 2012).

The chemical reaction of ozone with NO (R9.1) also contributes to an apparent uptake of ozone within the canopy. For the Waldstein site, both NO emissions from the soil and anthropogenic NO sources are quite small, and NO mixing ratios are typically well below 1 ppb. Nevertheless, the conversion of NO to NO_2 might contribute to apparent ozone deposition, in particular when the photolysis reaction of NO_2 (R9.2) is efficiently suppressed in the dark canopy. In fact, during dark periods without solar radiation, only ozone deposition was derived from a gradient approach, while also positive ozone fluxes (apparent emission) were observed when high NO concentrations and sunlight created an ozone sink above the canopy (Tsokankunku 2014).

Above the canopy, observed NO fluxes are mostly negative indicating efficient uptake within the canopy. Below the canopy, most of the NO emitted from the soil (e.g., Bargsten et al. 2010) is oxidized by O_3 in the first meter above the forest floor. This reaction acts as a below-canopy or in-canopy source of NO_2, which results in above-canopy emission fluxes of NO_2. NO_2 can be released from the canopy because NO_2 photolysis is strongly reduced in the dark canopy and because uptake by the spruce needles is quite low (Breuninger et al. 2012, 2013). Obviously, the distribution and magnitudes of the biological and chemical sources and sinks of NO and NO_2 have to be taken into account when comparing measurements of fluxes and concentration differences of these reactive trace gases.

9.3.1.3 Fluxes of Additional Reactive Trace Gases

Additional chemical reactions, e.g., the oxidation of NO_2 with OH, the reaction of NO with organic peroxy radicals, or the reaction of ozone with volatile organic compounds, expand the reactions of the chemical triad NO-NO_2-O_3 and can act as alternative sinks (or sources) of nitrogen oxides and ozone. Table 9.4 provides an overview of exchange fluxes of additional trace gases observed at the Waldstein site.

During daytime, photolysis of NO_2 competes with the reaction of NO_2 with the OH radical, which produces nitric acid (HNO_3). At the Waldstein-Weidenbrunnen site, mean HNO_3 concentrations of 32 nmol m^{-3} were reported for measurements in May 2002 (Pryor and Klemm 2004) and mean concentrations of 14 nmol m^{-3} as well as maximum concentrations of 69 nmol m^{-3} during EGER IOP1 (Wolff et al. 2010b). Pryor and Klemm (2004) calculated mean HNO_3 deposition fluxes of -1.5 nmol m^{-2} s^{-1} during daytime, ranging from roughly -7 to $+1$ nmol m^{-2} s^{-1}.

Table 9.3 Overview of observed trace gas fluxes at the Waldstein site: ozone and nitrogen oxides

Trace gas	Method	Height (m)	Specification	Flux (nmol m^{-2} s^{-1})	Reference
O_3	EC	32	Daily mean	−3 … −14	Klemm and Mangold (2001)
O_3	EC	32	Median	−0.5 … −8.6	Klemm et al. (2004)
O_3	EC	32		−25 … 0	Tsokankunku (2014)
O_3	GRAD	32/25		−10 … +10	Tsokankunku (2014)
O_3	EC	32	Daytime mean	−11.0	Zhu et al. (2009)
O_3	EC	32	Nighttime mean	−5.2	Zhu et al. (2009)
O_3	EC	32 (forest)	Median	−11.0	Voß (2015)
O_3	EC	17	Daytime mean	−7.0	Zhu et al. (2009)
O_3	EC	17	Nighttime mean	−3.0	Zhu et al. (2009)
O_3	EC	5.5 (clearing)	Median	−7.5	Voß (2015)
O_3	EC	1		−2.5 … 0	Tsokankunku (2014)
O_3	GRAD	1/0.005		−2.5 … 0	Tsokankunku (2014)
O_3	EC	1	Daytime mean	−0.8	Zhu et al. (2009)
O_3	EC	1	Nighttime mean	−0.5	Zhu et al. (2009)
NO	EC	32		−1.75 … 0	Tsokankunku (2014)
NO	GRAD	32/25		−1.75 … 0	Tsokankunku (2014)
NO	GRAD	1/0.005		+0.1 … +0.45	Tsokankunku (2014)
NO_2	EC	32		0 … +2	Tsokankunku (2014)
NO_2	GRAD	32/25		−2 … +2	Tsokankunku (2014)
NO_2	GRAD	1/0.005		−0.2 … +0.3	Tsokankunku (2014)

Table 9.4 Overview of observed trace gas fluxes at the Waldstein site: reactive nitrogen compounds, peroxides, and volatile organic compounds. Total NO_3^- and total NH_4^+ represent sum of trace gas and aerosol fluxes

Trace gas	Method	Height (m)	Specification	Flux (nmol m^{-2} s^{-1})	Reference
HNO_3	REA	32	Daytime mean	−1.5	Pryor et al. (2003), Pryor and Klemm (2004)
Total NO_3^-	GRAD	30.9/24.4	Monthly mean (September 2007)	−4.7	Wolff et al. (2010a, 2010b)
Total NH_4^+	GRAD	30.9/24.4	Monthly mean	−2.9	Wolff et al. (2010a, 2010b)
H_2O_2	REA	32	Daily mean	−0.8 ± 0.3	Valverde-Canossa et al. (2006)
MHP	REA	32	Daily mean	−0.03 ± 0.03	Valverde-Canossa et al. (2006)
HMHP	REA	32	Daily mean	−0.7 ± 0.5	Valverde-Canossa et al. (2006)
Isoprene	REA	32	Daytime max	up to +7	Steinbrecher et al. (2004)
Isoprene	REA	32	Daytime max	+1 to +1.5	Graus et al. (2006)
Isoprene	REA	32	Daytime max	+4.1 ± 0.8	Schmitt (2013)
Monoterpenes	REA	32	Daytime max	up to +5	Steinbrecher et al. (2004)
Monoterpenes	REA	32	Daytime max	+2	Graus et al. (2006)
Monoterpenes	REA	32	Daytime max	+5.5 ± 1.4	Schmitt (2013)

Cases of positive HNO_3 fluxes were observed in the morning hours and occurred together with positive ozone fluxes. This was interpreted as an indication of chemically induced flux divergence involving the NO-NO_2-O_3 triad. Apart from HNO_3 production by the reaction of NO_2 and OH, HNO_3 may be formed by repartitioning of ammonium nitrate or by hydrolysis of N_2O_5 in wet surface films on needles (Finlayson-Pitts and Pitts 2000). This indicates a non-negligible influence of gas-particle partitioning and the coupling of gaseous and aqueous phase chemistry on the concentrations and fluxes of reactive nitrogen species.

Wolff et al. (2010b) used a gradient approach to quantify the total ammonium (NH_3/NH_4^+) and the total nitrate (HNO_3/NO_3^-) exchange fluxes at the canopy top. When considering the sum of the gas and particle phases, repartitioning between the phases does not affect the total concentrations and fluxes. The total concentrations are conserved, and thus, the gradient approach for total ammonium and nitrate fluxes is less prone to flux divergence due to chemical reactions than for the individual compounds. Both total ammonium and total nitrate concentrations were dominated by the particulate phase. The mean total ammonium flux was -4.7 nmol m^{-2} s^{-1} with maximum daytime deposition fluxes up to -36 nmol m^{-2} s^{-1}. For total nitrate, the mean flux was -2.9 nmol m^{-2} s^{-1} and maximum daytime deposition fluxes up to -19 nmol m^{-2} s^{-1}. Both the total ammonium and nitrate fluxes were generally larger during sunny periods and smaller during cooler and more humid conditions. The total ammonium fluxes even showed emission events from wet or drying surfaces, while the total nitrate fluxes were always negative. This indicates that even though the total concentrations are not influenced by phase partitioning, the different deposition behavior of gaseous and particulate species is obviously reflected in changes of the total exchange fluxes.

Wolff et al. (2010b) point out that the exchange of reactive species seems not to be limited by any surface resistance. This is supported by REA flux measurements of hydrogen peroxide (H_2O_2) during the BEWA campaign in July 2001 (Valverde-Canossa et al. 2006). With maximum H_2O_2 mixing ratios of 1 ppb and less than 200 ppt of individual organic peroxides, Valverde-Canossa et al. (2006) observed daily mean H_2O_2 deposition fluxes of -0.8 ± 0.3 nmol m^{-2} s^{-1}, daily mean fluxes of hydroxymethyl hydroperoxide (HMHP) of -0.7 ± 0.5 nmol m^{-2} s^{-1}, and daily mean fluxes of methyl hydroperoxide (MHP) of -0.03 ± 0.03 nmol m^{-2} s^{-1}. During daytime, high deposition velocities suggest a negligible surface uptake resistance for H_2O_2, such that turbulent transport controls its surface exchange. In contrast, significantly smaller deposition velocities were observed for MHP indicating a significant surface uptake resistance. For HMHP, the REA measurements showed mainly deposition fluxes, while concentration profiles suggested in-canopy chemical production by reaction of ozone with alkenes. Such ozonolysis reactions within the canopy are also expected to affect the surface exchange of H_2O_2 and other organic peroxides, especially at nighttime.

With typical time scales of hours to days, H_2O_2 production by recombination of HO_2 is not expected to affect its turbulent transport with typical time scales in the order of minutes. However, laboratory studies (e.g., Hasson et al. 2001) suggest that H_2O_2 production from ozonolysis of alkenes can considerably influence the surface

exchange of H_2O_2. For MHP, in contrast, the yield from ozonolysis of alkenes is generally low, and typical time scales for MHP production and loss reactions are several hours.

The spruce trees at the Waldstein site are an important biogenic source of volatile organic compounds (VOC) including monoterpenes, isoprene, and other alkenes. Steinbrecher et al. (2004) reported maximum daytime canopy fluxes of isoprene up to +7 nmol m^{-2} s^{-1} and up to +5 nmol m^{-2} s^{-1} for the sum of monoterpenes derived from relaxed eddy accumulation with proton transfer reaction mass spectrometry (PTR-MS) in a case study in July 2001 during the BEWA field campaign. For the same field campaign, Graus et al. (2006) compared VOC canopy fluxes derived from REA PTR-MS and from a combination of REA and gas chromatography (REA GC). Both techniques agreed well during daytime with maximum isoprene fluxes up to +1.5 nmol m^{-2} s^{-1} and maximum monoterpene fluxes of +2.5 to +3 nmol m^{-2} s^{-1}. At night, negative monoterpene fluxes up to −1.5 nmol m^{-2} s^{-1} were obtained from the REA GC technique, while REA PTR-MS fluxes were close to zero.

The observed daytime fluxes were found to be consistent with plant emission fluxes derived from enclosure measurements on the branch level. Grabmer et al. (2006) obtained a monoterpene standard emission rate of 0.50 μg C g^{-1} dwt h^{-1} (dwt, leaf dry weight) from their measurements, which result in maximum daytime fluxes of 2.3 nmol m^{-2} s^{-1} under the specific conditions during the observation period. The standard emission rate of isoprene was determined to be 0.32 μg C g^{-1} dwt h^{-1}, resulting in a maximum daytime isoprene flux of 2.1 nmol m^{-2} s^{-1}. It has to be kept in mind that some of the volatile organic compounds emitted from the spruce needles are removed from the atmosphere by chemical reaction within the canopy. Thus, only a fraction of the primarily emitted VOC is released from the canopy to the atmosphere above due to in-canopy oxidation during turbulent transport.

The VOC above-canopy fluxes observed during the BEWA field campaign are consistent with the canopy fluxes derived from REA sampling and offline GC analysis in July 2013 (Schmitt 2013). The daily maximum isoprene fluxes were +4.1 ± 0.8 nmol m^{-2} s^{-1}, and the daily maximum fluxes of the sum of five monoterpenes were +5.5 ± 1.4 nmol m^{-2} s^{-1}. By comparison with the VOC emission pattern expected for Norway spruce taken from the MEGAN model (Guenther et al. 2012), Schmitt (2013) concluded that the emissions of α-pinene, β-pinene, camphene, Δ3-carene, and limonene contribute about 80 % to the total monoterpene emissions at the Waldstein site. Typical concentrations of the sum of these five monoterpenes ranged from roughly 1 to 70 nmol m^{-3} in the measurement period from May to October 2013.

Figure 9.1 schematically summarizes the reactive trace gas fluxes observed at the Waldstein-Weidenbrunnen site. Obviously, the vegetation is an important biogenic source of volatile organic compounds, which may contribute to a chemical flux divergence of the $NO/NO_2/O_3$ triad (e.g., Vilà-Guerau de Arellano et al. 1993). A certain fraction of the primarily emitted VOCs will be transported across the canopy and contribute to the observed above-canopy emission flux. Another fraction will

be oxidized within the canopy and yield oxygenated VOC or peroxy radicals (RO_2). Peroxy radicals and the hydroperoxyl radical (HO_2) can form hydrogen peroxide (H_2O_2) and organic peroxides such as methyl hydroperoxide (MHP), which exhibit a deposition flux to the canopy. Above-canopy NO deposition and NO soil emissions indicate an efficient in-canopy sink for NO. Because NO surface uptake can be considered negligible, chemical reactions seem to be important sink processes. For example, the reaction of NO with OH may form nitrous acid (HONO). Within the dark canopy, the reaction of NO with ozone or with peroxy radicals is probably more important. In particular, even small mixing ratios of peroxy radicals in the ppt range may affect $NO/NO_2/O_3$ exchange fluxes because the reaction constant of NO with the hydroperoxyl and other peroxy radicals is about 500 times higher than the reaction constant of NO with ozone. Thus, the oxidation of NO to NO_2 by organic peroxy radicals may shift the concentration ratios of the $NO/NO_2/O_3$ triad and will contribute to ozone formation if NO_2 is subsequently photolyzed. NO_2 may be taken up by plants; however, above-canopy emission of NO_2 was typically observed. Also above the canopy, NO_2 may react with OH and form nitric acid (HNO_3), which exhibited deposition fluxes. Photochemical production is an important source of ozone above the canopy, which contributes to overall ozone deposition. In addition, ozone is an extremely important oxidant for many primarily emitted volatile organic compounds. For example, monoterpene ozonolysis yields a large variety of oxygenated volatile organic compounds, which may finally partition into the particle phase after several oxidation steps. Thus, organic compounds contribute to both sink and source processes of ozone, and differences in VOC concentrations within and above the canopy reflect a complex interplay of turbulent transport and chemical reactions.

9.3.2 Aerosol Flux Measurements

The Waldstein site is located in a semirural area, where local anthropogenic aerosol sources are marginal. A large fraction of secondary inorganic aerosol, i.e., aerosol compounds such as sulfate, nitrate, and ammonium that have partitioned into the particle phase by chemical reaction of precursor gases (e.g., SO_2, NO_x, NH_3, see Chap. 3), indicates aerosol aging during long-range transport and advection to the Fichtelgebirge mountains (Klemm 2004). Extended areas of forest stands with an increased surface roughness may enhance turbulent exchange and thus aerosol deposition to the forest. On the other hand, local and regional formation of secondary organic aerosol from oxidation products of biogenic volatile organic compounds can contribute substantially to aerosol number concentrations during new particle formation events (e.g., Held et al. 2004). Therefore, the forest may act as a net aerosol sink or source, and aerosol flux measurements are required to quantify the surface exchange of particulate matter.

9.3.2.1 Aerosol Number Fluxes

Eddy covariance measurements of aerosol number fluxes were carried out during the BEWA field campaign in 2001 and 2002 (Held and Klemm 2006). The combination of a sonic anemometer and a condensation particle counter yields the net exchange with respect to the aerosol number concentration across the measurement height 22 m agl. In July/August 2001, the median aerosol deposition flux was -6.4×10^6 m^{-2} s^{-1} for particles with diameters (D) larger than 11 nm and -13.9×10^6 m^{-2} s^{-1} for $D > 3$ nm. The 95 % quantile flux was -30.5×10^6 m^{-2} s^{-1} ($D > 11$ nm) and -69.2×10^6 m^{-2} s^{-1} ($D > 3$ nm). This is consistent with measurements in July/August 2002, when the median aerosol deposition flux was -9.4×10^6 m^{-2} s^{-1} ($D > 11$ nm) and -16.7×10^6 m^{-2} s^{-1} ($D > 3$ nm) and the 95 % quantile flux was -60.9×10^6 m^{-2} s^{-1} ($D > 11$ nm) and -92.4×10^6 m^{-2} s^{-1} ($D > 3$ nm). Obviously, the net aerosol exchange is typically directed toward the surface. Eighty-six percent of the measurements in 2001 showed net deposition versus 14 % net emission. Similarly, net deposition was observed in 92 % of the flux measurements in 2002 compared with only 8 % of net emission.

Interestingly, the strongest deposition fluxes of more than 300×10^6 particles m^{-2} s^{-1} occurred during new particle formation events. Held et al. (2004) found strong indications that oxidation products of biogenic volatile organic compounds contribute considerably to secondary aerosol formation at the Waldstein site. However, if particles had been formed within the canopy, they were either too small to be detected with the ultrafine condensation particle counter (i.e., $D < 3$ nm), or the emission of these particles was obscured by stronger particle deposition. Alternatively, the time scale of VOC emission from the canopy by turbulent transport may have been faster than the time scale of the multistep oxidation mechanism of primarily released VOCs, which finally yielded condensable organic vapors that partition into the particle phase. Thus, secondary aerosol formation can act as a particle source above the forest canopy, while efficient turbulent deposition of nm-scale particles quickly removes these particles from the atmosphere. In other words, the forest acts both as a source of organic precursor gases for secondary aerosol formation and as a sink for freshly formed particles through turbulent deposition.

In August 2011, additional aerosol number flux measurements were carried out on the Köhlerloh clearing at 2.25 m agl with a Fast CPC (Wehner et al. 2011) ranging from -15.6×10^6 m^{-2} s^{-1} to $+9.1 \times 10^6$ m^{-2} s^{-1} and a median deposition flux of -3.3×10^6 m^{-2} s^{-1} (Kittler F., personal communication). Again, net aerosol deposition was clearly predominant.

9.3.2.2 Size-Resolved Number Fluxes

When comparing particles with diameters larger than 3 nm vs. 11 nm, significantly larger deposition fluxes of the smallest particle fraction are evident. These differences can be attributed to the particles in the diameter range between 3 nm

and 11 nm. This particle fraction typically contributes less than 25 % to the total number concentration; however, the contribution to the total deposition flux is frequently more than 50 % (Held and Klemm 2006). In fact, the deposition velocity v_d, calculated by dividing the negative aerosol flux by the aerosol number concentration, is significantly larger for $D > 3$ nm than for $D > 11$ nm. This size dependence of aerosol deposition is expected from theoretical descriptions of particle motion in the atmosphere: Small particles ($D < 100$ nm) are efficiently removed by diffusional processes, whereas large particles ($D > 1$ μm) are removed by sedimentation. In the diameter range from 100 nm to 1 μm, the so-called accumulation mode, the efficiency of dry deposition exhibits a minimum.

Moreover, bidirectional aerosol number fluxes were observed at the Waldstein-Weidenbrunnen site, i.e., aerosol deposition fluxes in one size range and simultaneously aerosol emission fluxes in another size range. As an example, Fig. 9.2a shows the diurnal cycle of aerosol number fluxes for two different diameter ranges on 12 July 2002 measured during the BEWA field campaign. The corresponding temporal evolution of the aerosol size distribution (Fig. 9.2b) indicates a new particle formation event. The buoyancy flux (Fig. 9.2c) shows a typical diurnal cycle with slightly negative values during the night and well-developed turbulence during the day.

The aerosol fluxes in Fig. 9.2a represent the total number fluxes of all particles with a diameter larger than 11 nm ($D > 11$ nm) versus $D > 3$ nm. Obviously, at nighttime the aerosol fluxes are close to zero in both diameter ranges. However, in the morning hours around 09:00 AM, the net aerosol fluxes of the measurements including the smaller particle fraction ($D > 3$ nm) become negative, while the net aerosol fluxes for $D > 11$ nm become positive. This indicates strong aerosol deposition of very small particles and at the same time aerosol emission of larger particles. Indeed, the particle fraction in the diameter range from 3 nm to 11 nm contributes strongly to the flux measurement for $D > 3$ nm. Therefore, the net aerosol emission measured for $D > 11$ nm was obscured by strong deposition of particles from 3 nm to 11 nm. This also suggests different source and sink distributions for different aerosol size fractions.

Recently, Deventer et al. (2015) carried out size-resolved eddy covariance aerosol flux measurements in the diameter range from 6 nm to 1.4 μm at a height of 32 m agl. The overall net deposition flux was -41×10^6 m^{-2} s^{-1}. However, the size-resolved aerosol fluxes were highly variable with respect to magnitude and direction. About 30 % of the quality-assured net fluxes were positive, and bidirectional fluxes were observed on a regular basis. Typically, the smallest particle size fractions exhibited the largest fraction of emission periods. In contrast, the net fluxes of accumulation mode particles with diameters larger than 0.2 μm were mostly negative. These observations may be explained either by true bidirectional aerosol exchange due to different locations of the sources of different aerosol size fractions or by evaporation of ammonium nitrate aerosol, which may be misleadingly interpreted as an emission flux. Chemically speciated aerosol flux measurements may be helpful to support one or the other explanation.

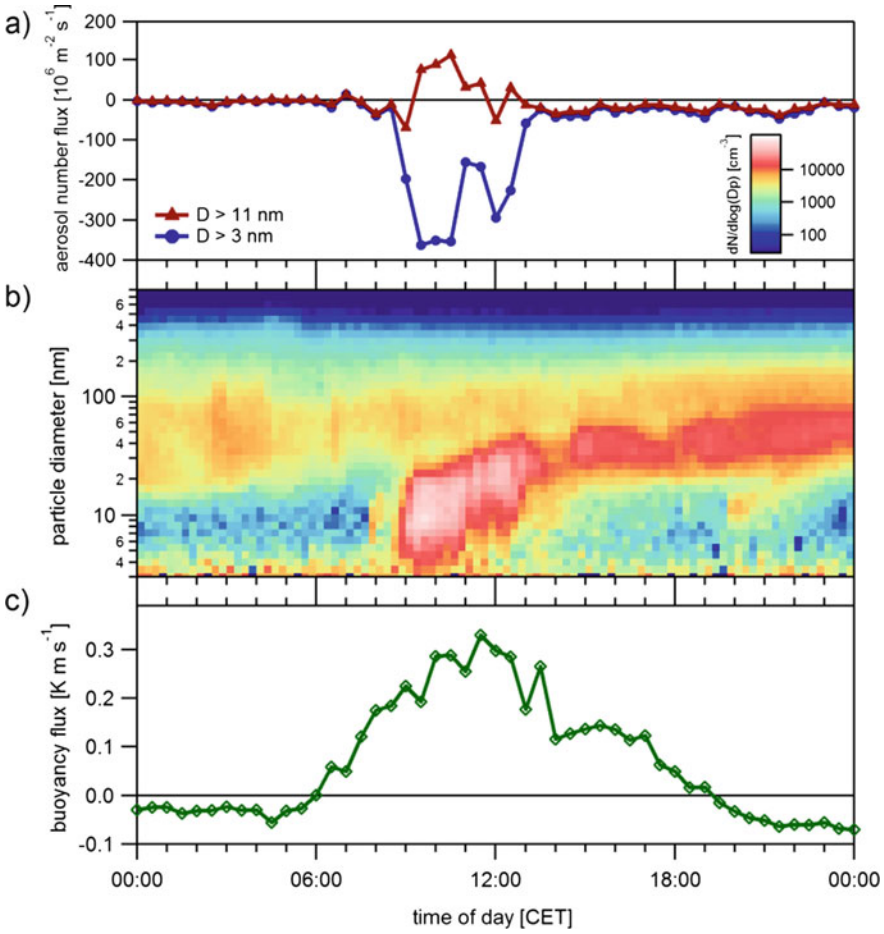

Fig. 9.2 An example of (**a**) bidirectional aerosol number fluxes, (**b**) the corresponding evolution of the aerosol size distribution, and (**c**) buoyancy fluxes observed on 12 July 2002

9.3.2.3 Chemically Speciated Aerosol Fluxes

The gradient measurements of total ammonium (NH_3/NH_4^+) and total nitrate (HNO_3/NO_3^-) exchange fluxes at the canopy top were already discussed in Sect. 9.3.1 (Wolff et al. 2010b). The mean total ammonium flux was -4.7 nmol m^{-2} s^{-1} and the mean total nitrate flux was -2.9 nmol m^{-2} s^{-1}. Since both total ammonium and total nitrate concentrations were dominated by the particulate phase, Wolff et al. (2010b) presumed that the particulate phase also dominates the observed deposition fluxes, at least for total nitrate. If this assumption holds, the total ammonium and nitrate deposition fluxes do not directly support (nor disprove) ammonium nitrate evaporation in the canopy. However, Held et al. (2003) used a combination

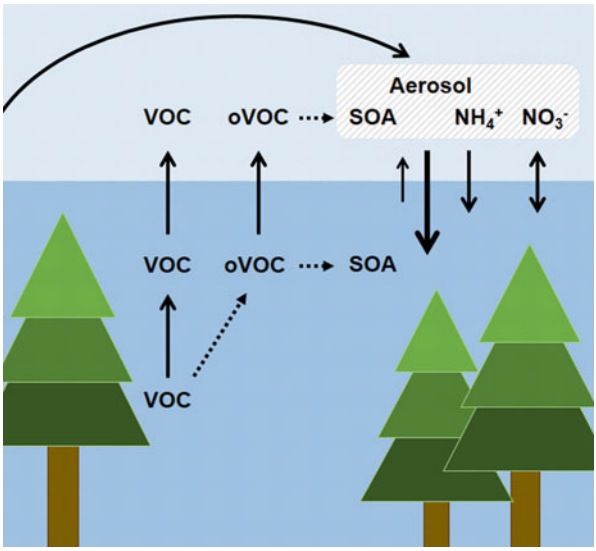

Fig. 9.3 Schematic representation of the interaction of aerosol fluxes and VOC chemistry at the Waldstein site (oVOC, oxygenated VOC; SOA, secondary organic aerosol); *solid arrows* indicate transport processes; *broken arrows* represent chemical reaction mechanisms

of irregular disjunct eddy sampling and single particle analysis by aerosol mass spectrometry and determined particulate nitrate emission with a confidence of 89 % in a case study at the Waldstein-Weidenbrunnen site.

Figure 9.3 summarizes the interactions of VOC emission and oxidation with secondary aerosol formation and aerosol transport at the Waldstein site. In most cases, aerosol deposition to the canopy is dominant, especially during periods of secondary aerosol formation, e.g., from oxidation products of biogenic VOC. In addition, aerosol that underwent aging during regional transport contributes to inorganic aerosol deposition. However, brief aerosol emission periods and bidirectional fluxes of different aerosol size fractions have been observed. It remains an open question whether these observations are true emission events or related to phase transitions of semi-volatile aerosol species such as ammonium nitrate or semi-volatile organic compounds.

9.3.3 Comparison of Flux Observations and Models

It is instructive to compare the observed trace gas and aerosol fluxes with flux parameterizations or flux models in order to evaluate the underlying process understanding.

For ozone deposition to tall vegetation, one-layer models with a simplified representation of the turbulent transport and the vegetation surfaces (big-leaf models) have been widely used. Klemm and Mangold (2001) compared ozone fluxes measured by eddy covariance at the Waldstein-Weidenbrunnen site with a simple big-leaf model. The measured daily average ozone deposition fluxes up to

−14 nmol m^{-2} s^{-1} were stronger than the modeled values, which ranged up to −6 nmol m^{-2} s^{-1}. Interestingly, both the modeled ozone mixing ratios and the modeled ozone deposition velocities, and thus, the modeled ozone fluxes, declined from May to October. In contrast, no clear seasonality was found for the measured fluxes, except for more frequent strong nocturnal fluxes toward the end of October. The discrepancy between the model and the measurements was explained by more efficient surface deposition compared to the model parameterization.

Schröter et al. (2002) emphasized the importance of ozone surface deposition by comparing ozone mixing ratios measured with UV absorption analyzers at the ground and with a LIDAR slightly above the ground. They found good agreement for ozone measurements 52 m agl at the top of the Schneeberg mountain, while the LIDAR measurements were systematically higher than the ground-based measurements at the Waldstein site and in the Weißenstadt basin. This difference was explained by ozone surface deposition and − in the case of the Weißenstadt basin − additional advection of ozone-depleted air.

A more detailed analysis of the diurnal cycles of measured and modeled ozone fluxes (Klemm et al. 2004) showed a general agreement of the magnitude of the median flux values (measured, up to −8.6 nmol m^{-2} s^{-1}; modeled, up to −9 nmol m^{-2} s^{-1}). However, large differences of the modeled fluxes during daytime and night, driven by a low stomatal resistance during the day versus closed stomata and a high cuticular resistance at night, do not reflect the measured diurnal cycles of the ozone flux. At night, the measured ozone deposition fluxes were unexpectedly large and not adequately parameterized in the ozone deposition model. Because stomata are closed and the stomatal uptake is strongly reduced at night, the large nighttime deposition fluxes suggest non-stomatal uptake. Both surface deposition and chemical reaction might contribute to this removal pathway. Deposition of ozone to vegetation surfaces has been studied extensively (e.g., Pilegaard et al. 1995; Fares et al. 2008). For example, ozone can react with plant waxes and with compounds deposited onto plant surfaces. In addition, the surface uptake of ozone is enhanced for wet leaves or needles (e.g., Fuentes et al. 1992; Zhang et al. 2002; Altimir et al. 2006), even though the water solubility of ozone is not large.

The surface wetness is often high at night, when humidity conditions within the canopy support the formation of liquid films on the spruce needles (e.g., Klemm et al. 2002). However, the parameterization of enhanced ozone surface deposition as a function of humidity or leaf surface wetness is not yet quantitative. This is corroborated by Voß (2015), who found a clear dependence of the deviation of measurements and model results on relative humidity when comparing ozone fluxes observed at the Waldstein site and modeled using the multilayer canopy-chemistry exchange model (MLC-CHEM).

Ganzeveld et al. (2006a) evaluated the H_2O_2 and organic peroxide exchange fluxes observed by Valverde-Canossa et al. (2006) with a single-column model (SCM) version of the coupled chemistry-climate model ECHAM4 adjusted to the Waldstein-Weidenbrunnen site (Ganzeveld et al. 2006b). From a comparison of the measured and simulated H_2O_2 fluxes, the observed H_2O_2 surface uptake resistance

was found to be much smaller than estimated by the model. However, even when using a very small surface uptake resistance in the model, the simulated H_2O_2 fluxes were still lower than the observed fluxes due to an underestimation of the turbulent transport. At night, when turbulent mixing was suppressed, non-stomatal uptake and chemical transformations, which are linked to the $NO/NO_2/O_3$ triad, were key controls of H_2O_2 mixing ratios. This intercomparison study of peroxide measurements and model simulations emphasizes the important role of turbulent transport, which controls the deposition of peroxides that are chemically produced above the canopy. At the same time, the production of peroxides depends on the emission flux of biogenically emitted organic precursor gases, e.g., a potential contribution to H_2O_2 production from terpene ozonolysis.

Forkel et al. (2006) applied the one-dimensional canopy-chemistry model CACHE to the Waldstein spruce canopy during the BEWA field experiments in order to compare measured and simulated VOC emission fluxes. The general levels of both the mixing ratios and the fluxes of isoprene and monoterpenes were in good agreement between the observations and the model simulations. However, the model could not reproduce the observed strong fluctuations, which have been attributed to the patchiness of the forest canopy. The model simulations suggested that the above-canopy VOC emission fluxes were about 10–15 % lower than the primary emission fluxes from the branches due to chemical reactions within the canopy. For individual species such as limonene, the above-canopy emission fluxes were reduced by up to 30 % due to the higher reactivity of these species. Furthermore, the simulations indicated that daytime VOC oxidation was not only due to ozone and OH radicals but also due to nitrate radicals in the lower part of the canopy.

The VOC emission fluxes measured during the BEWA field experiments at the Waldstein-Weidenbrunnen site were also used to validate a regional-scale semi-empirical BVOC (seBVOC) emission model (Smiatek and Steinbrecher 2006). For validation, the seBVOC model was run in point mode. The simulated diurnal cycles of isoprene and monoterpene fluxes resembled the observations. Taking into account the reduction of primary emission fluxes due to chemical reactions, the measured and simulated fluxes agreed within a factor of less than two for isoprene, and a factor of three for monoterpenes, which is considered to be well within the range of other upscaling studies. Further, it was noted that the emission potentials observed at the Waldstein site were at the lower end of values reported for Norway spruce.

With respect to aerosol deposition, Peters and Eiden (1992) introduced a size-dependent parameterization of the dry deposition velocity of aerosol particles to a spruce forest, which was applied to a spruce stand in Wülfersreuth, close to the Waldstein site. Later, Peters and Bruckner-Schatt (1995) extended this model in order to calculate dry deposition velocities of both gases and particles. Held et al. (2006) evaluated net aerosol number flux measurements together with a size-resolved particle deposition model by Zhang et al. (2001) based on the Slinn (1982) approach. In most cases, the model simulations were in fair agreement with the eddy covariance measurements. The size-resolved aerosol deposition flux was derived from a combination of the particle deposition model and size distribution measurements. The results indicated that the aerosol number flux was controlled by

ultrafine particles with diameters smaller than 50 nm, whereas the estimated aerosol mass flux was dominated by accumulation mode particles.

A more sophisticated simulation of aerosol deposition fluxes was carried out with the one-dimensional SOLVEG model (Katata et al. 2011). The net aerosol number fluxes calculated with SOLVEG agreed well with the observed fluxes. Size-resolved deposition velocities agreed well with measurements for diameters larger than 1 μm and for diameters smaller than 100 nm. However, for the accumulation mode, the calculated deposition velocities were significantly smaller than the measured ones. This discrepancy may be (partly) explained by flux divergence induced by a phase transition of semi-volatile aerosol species.

9.4 Conclusions

Over the last 20 years, reactive trace gas fluxes including ozone, nitrogen oxides, and volatile organic compounds as well as aerosol number and mass fluxes have been measured at the Waldstein-Weidenbrunnen site. The atmosphere-surface exchange of reactive trace gases and aerosols is influenced by turbulent transport, chemical reactions, and phase transitions. When interpreting turbulent flux measurements of reactive species, one should always evaluate the potential of chemical reactions to act as source and sink processes. For example, ozone formed outside of the canopy by photochemistry is removed from the atmosphere by turbulent deposition to surfaces, by stomatal and non-stomatal uptake, and by reaction with NO, which is also a sink for nitric oxide and a source for nitrogen dioxide. This in-canopy NO sink explains the observed flux convergence, with NO deposition above the canopy and at the same time NO soil emission close to the ground (see also Chap. 8). The same chemical reaction R9.1 acts as an in-canopy source of NO_2. In fact, NO_2 emission fluxes are observed above the canopy because NO_2 photolysis is strongly reduced within the canopy due to shading, and plant uptake of NO_2 has been shown to be quite small at the Waldstein site. At the same time, plant surfaces are important for ozone removal, which is corroborated by the observation of reduced ozone deposition fluxes in a clearing compared to the undisturbed forest canopy. One might speculate that a future increase in disturbance events such as wind storms will reduce the areas of undisturbed canopy and thus reduce ozone deposition to plant surfaces.

In order to assess the interaction of turbulent transport and chemistry, the characteristic turbulent and chemical time scales must be compared. For example, the Damköhler number, i.e., the ratio of the turbulent transport time and the chemical reaction time, has been evaluated for the $NO/NO_2/O_3$ triad (e.g., Lenschow 1982; Tsokankunku 2014; Plake et al. 2015) or VOC exchange fluxes (e.g., Rinne et al. 2012). However, canopy coupling regimes (see Chaps. 6 and 19) add an additional constraint on the potential for chemical reactions of compounds from different sources. For example, canopy decoupling may efficiently suppress the transport of ozone into the lower canopy and as a result shut down NO_2 production due to reaction of ozone with NO from soil emissions. Therefore, vertical profiles of con-

centration and flux measurements are required to help identify and quantify multiple sources and sinks of reactive species and chemically induced flux divergence.

Considering the turbulent aerosol exchange, it can be concluded that the Waldstein forest canopy typically acts as a net sink with respect to particle number but may also act as a net source of particle mass. Both an increased surface roughness and the presence of needle surfaces promote turbulent deposition of nm-scale particles to the canopy. At the same time, VOCs are emitted from the canopy that potentially contribute to new particle formation. If particle formation by multiple oxidation reactions of primarily emitted VOCs is faster than the vertical turbulent transport of VOCs to the canopy top, above-canopy particle emission fluxes are expected. Freshly formed particles exhibit diameters of less than 10 nm, and indeed, the smallest particle size fractions show the largest fraction of emission periods. Overall, however, net deposition number fluxes prevail at the Waldstein site, i.e., new particles are typically formed by secondary aerosol formation above the canopy and efficiently removed by deposition to the canopy. While it is still difficult to directly quantify the turbulent mass exchange of particle-borne nutrients or pollutants, dry deposition of compounds such as sulfate and nitrate must be assessed and contrasted with wet deposition (see Chap. 3). The presented chemically speciated aerosol flux measurements help to constrain atmospheric budgets and cycles of nitrogen. Nevertheless, there are still technical limitations and conceptual challenges that need to be tackled in order to address yet unresolved questions with respect to reactive trace gas and aerosol fluxes within and above tall vegetation.

Acknowledgments The research summarized in this chapter was funded by the Federal Ministry of Education, Science, Research and Technology (BMBF, PT BEO 51-0339476 C, and PT UKF 07ATF25) and the German Science Foundation (DFG) in the first EGER period (IOP1/2: ME 4100/4-1) and in the second EGER period (IOP3: PAK 446), as well as HE 5214/4-1. The authors acknowledge support by all participants of the BEWA 2000 and EGER field experiments and by the technical staff of the University of Bayreuth. Scientific contributions and instrumental support by Otto Klemm (WWU Münster, Germany) are gratefully acknowledged. The 2013 VOC REA flux measurements were supported by A. A. Turnipseed and A. B. Guenther, then at the National Center for Atmospheric Research (Boulder, Colorado, USA).

References

Altimir N, Kolari P, Tuovinen J-P, Vesala T, Bäck J, Suni T, Kulmala M, Hari P (2006) Foliage surface ozone deposition: a role for surface moisture? Biogeoscience 3:209–228

Bargsten A, Falge E, Pritsch K, Huwe B, Meixner FX (2010) Laboratory measurements of nitric oxide release from forest soil with a thick organic layer under different understory types. Biogeoscience 7:1425–1441

Boucher O, Randall D, Artaxo P, Bretherton C, Feingold G, Forster P, Kerminen V-M, Kondo Y, Liao H, Lohmann U, Rasch P, Satheesh SK, Sherwood S, Stevens B, Zhang XY (2013) Clouds and aerosols. In: Stocker TF, Qin D, Plattner G-K, Tignor M, Allen SK, Boschung J, Nauels A, Xia Y, Bex V, Midgley PM (eds) Climate change 2013: the physical science basis. Contribution of working group I to the fifth assessment report of the Intergovernmental Panel on Climate Change. Cambridge University Press, Cambridge, pp 571–657

Breuninger C, Oswald R, Kesselmeier J, Meixner FX (2012) The dynamic chamber method: trace gas exchange fluxes (NO, NO_2, O_3) between plants and the atmosphere in the laboratory and in the field. Atmos Meas Tech 5:955–989

Breuninger C, Meixner FX, Kesselmeier J (2013) Field investigations of nitrogen dioxide (NO_2) exchange between plants and the atmosphere. Atmos Chem Phys 13:773–790

Deventer MJ, Held A, El-Madany TS, Klemm O (2015) Size-resolved eddy covariance fluxes of nucleation to accumulation mode aerosol particles over a coniferous forest. Agric Forest Meteorol 214–215:328–340

Fares S, Loreto F, Kleist E, Wildt J (2008) Stomatal uptake and stomatal deposition of ozone in isoprene and monoterpene emitting plants. Plant Biol 10:44–54

Finlayson-Pitts BJ, Pitts JN (2000) Chemistry of the upper and lower troposphere. Academic Press, San Diego, CA, p. 969

Foken T, Meixner FX et al (2012) Coupling processes and exchange of energy and reactive and non-reactive trace gases at a forest site – results of the EGER experiment. Atmos Chem Phys 12:1923–1950

Forkel R, Rappenglück B, Steinbrecher R, Klemm O, Held A, Graus M, Grabmer W, Hansel A (2006) Trace gas exchange and gas phase chemistry in a Norway spruce forest: a study with a coupled 1-dimensional canopy atmospheric chemistry emission model. Atmos Environ 40:S28–S42

Fuentes JD, Gillespie TJ, Den Hartog G, Neumann HH (1992) Ozone deposition onto a deciduous forest during dry and wet conditions. Agric Forest Meteorol 62:1–18

Ganzeveld L, Valverde-Canossa J, Moortgat GK, Steinbrecher R (2006a) Evaluation of peroxide exchanges over a coniferous forest in a single-column chemistry-climate model. Atmos Environ 40:S68–S80

Ganzeveld L, Klemm O, Rappenglück B, Valverde-Canossa J (2006b) Evaluation of meteorological parameters over a coniferous forest in a single-column chemistry-climate model. Atmos Environ 40:S21–S27

Grabmer W, Kreuzwieser J, Wisthaler A, Cojocariu C, Graus M, Rennenberg H, Steigner D, Steinbrecher R, Hansel A (2006) VOC emissions from Norway spruce (*Picea abies* L. [Karst]) twigs in the field—Results of a dynamic enclosure study. Atmos Environ 40:S128–S137

Graus M, Hansel A, Wisthaler A, Lindinger C, Forkel R, Hauff K, Klauer M, Pfichner A, Rappenglück B, Steigner D, Steinbrecher R (2006) A relaxed-eddy-accumulation method for the measurement of isoprenoid canopy-fluxes using an online gas-chromatographic technique and PTR-MS simultaneously. Atmos Environ 40:S43–S54

Guenther AB, Jiang X, Heald CL, Sakulyanontvittaya T, Duhl T, Emmons LK, Wang X (2012) The Model of Emissions of Gases and Aerosols from Nature version 2.1 (MEGAN2.1): an extended and updated framework for modeling biogenic emissions. Geosci Model Dev 5:1471–1492

Güsten H, Heinrich G (1996) On-line measurements of ozone surface fluxes: Part I. Methodology and instrumentation. Atmos Environ 30:897–909

Hasson AS, Ho AW, Kuwata KT, Paulson SE (2001) Production of stabilized Criegee intermediates and peroxides in the gas phase ozonolysis of alkenes. 2. Asymmetric and biogenic alkenes. J Geophys Res 106:34143–34153

Held A, Klemm O (2006) Direct measurement of turbulent particle exchange with a twin CPC eddy covariance system. Atmos Environ 40:S92–102

Held A, Hinz K-P, Trimborn A, Spengler B, Klemm O (2003) Towards direct measurement of turbulent vertical fluxes of compounds in atmospheric aerosol particles. Geophys Res Lett 30:2016. doi:10.1029/2003GL017854

Held A, Nowak A, Birmili W, Wiedensohler A, Forkel R, Klemm O (2004) Observations of particle formation and growth in a mountainous forest region in central Europe. J Geophys Res 109:D23204. doi:10.1029/2004JD005346

Held A, Nowak A, Wiedensohler A, Klemm O (2006) Field measurements and size-resolved model simulations of turbulent particle transport to a forest canopy. J Aerosol Sci 37:786–798

Karl T, Guenther A, Jordan A, Fall R, Lindinger W (2001) Eddy covariance measurement of biogenic oxygenated VOC emissions from hay harvesting. Atmos Environ 35:491–495

Katata G, Nagai H, Zhang L, Held A, Sera D, Klemm O (2011) Development of an atmosphere-soil-vegetation model for investigation of radioactive materials transport in the terrestrial biosphere. Prog Nuclear Sci Technol 2:530–537

Klemm O (2004) Trace gases and particles in the atmospheric boundary layer at the Waldstein site: present state and his historic trends. In: Matzner E (ed) Biogeochemistry of forested catchments in a changing environment, A German case study, Ecological studies, vol 172. Springer, Heidelberg, pp 45–58

Klemm O, Mangold A (2001) Ozone deposition at a forest site in NE Bavaria. Water Air Soil Poll: Focus 1:223–232

Klemm O, Milford C, Sutton MA, Spindler G, van Putten E (2002) A climatology of leaf surface wetness. Theor Appl Climatol 71:107–117

Klemm O, Mangold A, Held A (2004) Turbulent deposition of ozone to a mountainous forest ecosystem. In: Matzner E (ed) Biogeochemistry of forested catchments in a changing environment, A German case study, Ecological studies, vol 172. Springer, Heidelberg, pp 203–213

Klemm O, Held A, Forkel R, Gasche R, Kanter H-J, Rappenglück B, Steinbrecher R, Müller K, Plewka A, Cojocariu C, Kreuzwieser J, Valverde-Canossa J, Schuster G, Moortgat GK, Graus M, Hansel A (2006) Experiments on forest/atmosphere exchange: climatology and fluxes during two summer campaigns in NE Bavaria. Atmos Environ 40:S3–20

Lenschow DH (1982) Reactive trace species in the boundary layer from a micrometeorological perspective. J Meteor Soc Japan 60:472–480

Lerdau MT, Munger JW, Jacob DJ (2000) The NO_2 flux conundrum. Science 289:2291–2293

Lindinger W, Hansel A, Jordan A (1998) Proton-transfer reaction mass spectrometry (PTR-MS): on-line monitoring of volatile organic compounds at pptv levels. Chem Soc Rev 27:347–354

Müller M, Graus M, Ruuskanen TM, Schnitzhofer R, Bamberger I, Kaser L, Titzmann T, Hörtnagl L, Wohlfahrt G, Karl T, Hansel A (2010) First eddy covariance flux measurements by PTR-TOF. Atmos Meas Tech 3:387–395

Peters K, Bruckner-Schatt G (1995) The dry deposition of gaseous and particulate nitrogen compounds to a spruce stand. Water Air Soil Poll 85:2217–2222

Peters K, Eiden R (1992) Modelling the dry deposition velocity of aerosol particles to a spruce forest. Atmos Environ 26A:2555–2564

Pilegaard K, Jensen NO, Hummelshoj P (1995) Seasonal and diurnal variation in the deposition velocity of ozone over a spruce forest in Denmark. Water Air Soil Poll 85:2223–2228

Plake D, Sörgel M, Stella P, Held A, Trebs I (2015) Influence of meteorology and anthropogenic pollution on chemical flux divergence of the NO–NO_2–O_3 triad above and within a natural grassland canopy. Biogeoscience 12:945–959

Pryor SC, Klemm O (2004) Experimentally derived estimates of nitric acid dry deposition velocity and viscous sub-layer resistance at a conifer forest. Atmos Environ 38:2769–2777

Pryor SC, Barthelmie RJ, Jensen B, Jensen NO, Sörensen LL (2002) HNO_3 fluxes to a deciduous forest derived using gradient and REA methods. Atmos Environ 36:5993–5999

Pryor SC, Klemm O, Barthelmie R (2003) An investigation of the magnitude of resistance terms in dry deposition fluxes to a conifer forest. In: BACCI workshop on surface flux, micrometeorology and chemistry, Risø, 11–12 November 2003

Rinne J, Markkanen T, Ruuskanen TM, Petäjä T, Keronen P, Tang MJ, Crowley JN, Rannik U, Vesala T (2012) Effect of chemical degradation on fluxes of reactive compounds – a study with a stochastic Lagrangian transport model. Atmos Chem Phys 12:4843–4854

Schmitt SH (2013) Fluxes of monoterpenes from a spruce forest: establishing sampling and analytical procedures. MSc Thesis, University of Bayreuth, Germany

Schröter M, Obermeier A, Brüggemann D, Klemm O (2002) Application of a ground-based Lidar for studies of the dynamics of ozone in a mountainous basin. Environ Sci Pollut Res 9:381–384

Slinn WGN (1982) Predictions for particle deposition to vegetative surfaces. Atmos Environ 16:1785–1794

Smiatek G, Steinbrecher R (2006) Temporal and spatial variation of forest VOC emissions in Germany in the decade 1994–2003. Atmos Environ 40:S166–S177

Steinbrecher R, Klauer M, Hauff K, Stockwell R, Jaeschke W, Dietrich W, Herbert F (2000) Biogenic and anthropogenic fluxes of non-methane hydrocarbons over an urban-impacted forest, Frankfurter Stadtwald, Germany. Atmos Environ 34:3779–3788

Steinbrecher R, Rappenglück B, Hansel A, Graus M, Klemm O, Held A, Wiedensohler A, Nowak A (2004) Vegetation-atmospheric interactions: the emissions of biogenic volatile organic compounds (BVOC) and their relevance to atmospheric particle dynamics. In: Matzner E (ed) Biogeochemistry of forested catchments in a changing environment, A German case study, Ecological studies, vol 172. Springer, Heidelberg, pp 215–235

Trimborn A, Hinz K-P, Spengler B (2000) Online analysis of atmospheric particles with a transportable laser mass spectrometer. Aerosol Sci Technol 33:191–201

Tsokankunku A (2014) Fluxes of the NO-O_3-NO_2 triad above a spruce forest canopy in south-eastern Germany. PhD Thesis, University of Bayreuth, Germany

Valverde-Canossa J (2004) Sources and sinks of organic peroxides in the planetary boundary layer. PhD Thesis, Johannes Gutenberg Universität Mainz, Germany

Valverde-Canossa J, Ganzeveld L, Rappenglück B, Steinbrecher R, Klemm O, Schuster G, Moortgat GK (2006) First measurements of H2O2 and organic peroxides surface fluxes by the relaxed eddy-accumulation technique. Atmos Environ 40:S55–S67

Vilà-Guerau de Arellano J, Duynkerke PG, Builtjes PJH (1993) The divergence of the turbulent diffusion flux in the surface layer due to chemical reactions: the NO-O_3-NO_2 system. Tellus 45B:23–33

Voß L (2015) Measurements and modeling of ozone fluxes in and above Norway spruce canopies. PhD Thesis, Johannes Gutenberg University Mainz, Germany

Wehner B, Siebert H, Hermann M, Ditas F, Wiedensohler A (2011) Characterisation of a new Fast CPC and its application for atmospheric particle measurements. Atmos Meas Tech 4:823–833

Wolff V, Trebs I, Ammann C, Meixner FX (2010a) Aerodynamic gradient measurements of the NH_3-HNO_3-NH_4NO_3 triad using a wet chemical instrument: an analysis of precision requirements and flux errors. Atmos Meas Tech 3:187–208

Wolff V, Trebs I, Foken T, Meixner FX (2010b) Exchange of reactive nitrogen compounds: concentrations and fluxes of total ammonium and total nitrate above a spruce canopy. Biogeoscience 7:1729–1744

Zhang L, Gong S, Padro J, Barrie L (2001) A size-segregated particle dry deposition scheme for an atmospheric aerosol module. Atmos Environ 35:549–560

Zhang L, Brook JR, Vet R (2002) On ozone dry deposition – with emphasis on non-stomatal uptake and wet canopies. Atmos Environ 36:4787–4799

Zhu Z, Tsokankunku A, Plake D, Falge E, Foken T, Meixner FX (2009) Multi-level eddy covariance measurements for ozone fluxes above, within and below spruce forest canopy. In: Luers J, Foken T (eds) Proceedings of the international conference of atmospheric transport and chemistry in forest ecosystems. Arbeitsergebn, Univ Bayreuth, Abt Mikrometeorol. ISSN 1614–8916. 40:32